

Spin fluctuations in CuGeO_3 probed by light scattering

Haruhiko Kuroe, Jun-ichi Sasaki, and Tomoyuki Sekine

Department of Physics, Sophia University,

7-1 Kioi-cho, Chiyoda-ku, Tokyo 102, Japan

Naoki Koide, Yoshitaka Sasago, and Kunimitsu Uchinokura

Department of Applied Physics, The University of Tokyo,

7-3-1 Hongo, Bunkyo-ku, Tokyo 113, Japan

Masashi Hase

The Institute of Physical and Chemical Research (RIKEN),

2-1 Hirosawa, Wako-shi, Saitama 351-01, Japan

Abstract

We have measured temperature dependence of low-frequency Raman spectra in CuGeO_3 , and have observed the quasi-elastic scattering in the (c, c) polarization above the spin-Peierls transition temperature. We attribute it to the fluctuations of energy density in the spin system. The magnetic specific heat and an inverse of the magnetic correlation length can be derived from the quasi-elastic scattering. The inverse of the magnetic correlation length is proportional to $(T - T_{SP})^{1/2}$ at high temperatures. We compare the specific heat with a competing- J model. This model cannot explain quantitatively both the specific heat and the magnetic susceptibility with the same parameters. The origin of this discrepancy is discussed.

PACS numbers: 78.30.-j, 78.20.-e, 75.90.+w

1. INTRODUCTION

Hase, Terasaki, and Uchinokura¹ reported that the magnetic susceptibility in all directions in CuGeO_3 decreases exponentially below $T_{SP} = 14$ K, and they concluded that it is due to a spin-Peierls (SP) transition. In the SP phase, an energy gap between the singlet ground and the triplet excited states opens and a lattice dimerization is formed.² After this report, many experimental studies have been performed in this compound to reveal the nature of the SP phase. The magnetic excitations and the SP gap have been extensively studied by inelastic-neutron³ and Raman scattering.⁴ Moreover the lattice dimerization was observed below T_{SP} ,⁵⁻⁷ and then the SP transition was established in CuGeO_3 .

On the other hand, Hase, Terasaki, and Uchinokura¹ pointed out that the magnetic susceptibility above T_{SP} cannot be described quantitatively by Bonner-Fisher's theory⁸ based on an $S = 1/2$ one-dimensional (1D) Heisenberg antiferromagnetic (AF) Hamiltonian with a nearest-neighbor (nn) exchange interaction. Recently, Riera and Dobry⁹ and Castilla, Chakravarty, and Emery¹⁰ proposed independently for CuGeO_3 an $S = 1/2$ 1D Heisenberg model with the nearest- and next-nearest-neighbor (nnn) AF exchange interactions in the chain (a competing- J model). The Hamiltonian of this model is written as

$$\mathcal{H} = J \sum_{i=1}^N (\mathbf{S}_i \cdot \mathbf{S}_{i+1} + \alpha \mathbf{S}_i \cdot \mathbf{S}_{i+2}) , \quad (1)$$

where $J (> 0)$ and $\alpha (> 0)$ are the nn AF exchange interaction and the ratio of the nnn interaction to the nn one, respectively. In this model, if α is larger than a critical value α_c , an energy gap between the singlet ground and the triplet excited states appears without any lattice dimerization. α_c is estimated to be 0.2411.^{11,12} Riera and Dobry suggested that the model with $J = 160$ K and $\alpha = 0.36$ can explain the magnetic susceptibility above T_{SP} .⁹ On the other hand, Castilla, Chakrabarty, and Emery reported that the model with $J = 150$ K and $\alpha = 0.24$ can explain both the magnetic susceptibility above T_{SP} and a dispersion of magnetic excitations at low temperatures.¹⁰

In order to check the validity of this model, other experimental results will be compared

with this model. As is well known, the magnetic specific heat (C_m), as well as the magnetic susceptibility, is an important physical quantity. Therefore, it is necessary to measure accurately C_m at high temperatures. However, C_m at high temperatures has been poorly studied, although the anomalous specific heat around T_{SP} in CuGeO_3 was investigated in many experiments.^{13–19} Weiden *et al.*¹⁹ observed the specific heat below 300 K in polycrystalline CuGeO_3 using a continuous-heating adiabatic method. They obtained C_m after subtracting a calculated lattice specific heat from the observed one. The lattice specific heat was assumed to be written as a sum of Debye functions. They reported that C_m shows a broad maximum around 40 K. As we will describe below, our result contradicts theirs. As is well known, C_m at high temperatures cannot be obtained accurately by this method because effects of optical phonons, which play an important role in the specific heat at high temperatures, were not taken into account precisely.

It is noted that the quasi-elastic scattering is a powerful tool to derive precisely C_m especially at high temperatures. In our brief report,²⁰ a large tail near an incident laser line with a strong temperature dependence was observed at high temperatures in single-crystal CuGeO_3 , the profile in the Stokes and anti-Stokes scattering was fit to a Lorentzian curve. We assigned it to the quasi-elastic scattering due to spin-energy fluctuations. We can obtain roughly the magnetic specific heat from the quasi-elastic Raman scattering in CuGeO_3 , because the integrated intensity of the quasi-elastic scattering is proportional to $C_m T^2$ where T is the temperature.²¹ The quasi-elastic scattering was applied to some magnets such as a two-dimensional antiferromagnet FePS_3 ,²² and later a 1D antiferromagnet KCuF_3 .²³

In our brief report²⁰ we observed Raman spectra in both the Stokes and anti-Stokes regions at seven different temperatures. The Raman spectra, however, contained a weak component of the direct scattering, judging from the fact that a plasma line of the incident laser line appeared at -13.4 cm^{-1} . The quality of the sample was probably worse than that used in the present work. It is, of course, necessary to use high-quality samples in order to the effects of the direct scattering when we measure the quasi-elastic scattering. Then we did not obtain accurately the integrated intensity of the quasi-elastic scattering, in particular at

low temperatures. At low temperatures the intensity of the quasi-elastic scattering decreased in CuGeO_3 and it was considerably affected by the direct scattering, when we estimated the integrated intensity in our brief report.

Very recently, on the other hand, van Loosdreht *et al.*²⁴ measured Stokes Raman spectra with a backscattering geometry and proposed that the low-frequency Raman spectrum at high temperatures originated from the diffusive-type fluctuations in the four-spin time correlation functions. Richards and Brya²⁵ theoretically studied Raman scattering from the diffusive-type fluctuations in the spin system by using a four-spin time correlation function and obtained a result that the profile was described as a Gaussian-like line at $\omega=0$ at high temperatures. Therefore the model proposed by van Loosdreht *et al.* seems to contradict the interpretation for the quasi-elastic scattering in our brief report.²⁰

Therefore the careful and precise measurement of the low-frequency Raman spectrum in both the Stokes and anti-Stokes regions is needed in a high-quality sample in order to reveal clearly the origin of the quasi-elastic Raman scattering. In the present paper we shall obtain the magnetic specific heat precisely above T_{SP} and study effects of the nnn AF exchange interaction along the magnetic chain on the magnetic properties of CuGeO_3 .

2. EXPERIMENTAL DETAILS

A single crystal used in this study was made by a floating-zone method. The dimension of the crystal is $1.2 \times 1.8 \times 10.7 \text{ mm}^3$ parallel to the a , b , and c axes, respectively.²⁶ The single crystal has flat ac and bc faces. On the other hand, it is difficult to polish the ab face because of cleavage on the bc face. However, effects of local strain on the ab face were negligible when the light was incident and scattered on the ac and bc faces. The bc face was attached to the sample holder by dilute varnish.

Raman-scattering experiments were carried out using the 5145-Å line of an Ar^+ ion laser. The polarized quasi-elastic Raman scattering was measured in either a right-angle or a quasi-back scattering geometry. The detailed temperature dependence of the quasi-elastic

Raman scattering was measured in the right-angle scattering geometry. To eliminate plasma lines and to get a complete linear polarization, we made the laser light pass through a filter and a polarizer and then the laser light was incident on the sample in a cryostat. The light was incident on the *ac* face for the right-angle scattering and on the *bc* face for the quasi-back scattering. The scattered light was dispersed by a Jobin-Yvon U1000 double-grating monochromator and was detected by a photon counting system. The whole system is controlled by a microcomputer. To measure Raman spectra below room temperature, we used a closed-cycle cryostat. The temperature of the sample is controlled by a PID temperature controller. The temperature of the sample is equal to that of the sample holder within ± 0.1 K. Since the sample is transparent, the local temperature rise due to the incident light is negligible.

3. THEORIES

A. QUASI-ELASTIC SCATTERING

We summarize briefly the theory of the quasi-elastic light scattering in antiferromagnets. According to Halley's theory,²¹ the intensity of the quasi-elastic light scattering is given by the following Fourier component of the correlation function of the magnetic energy density:

$$I(\omega) = \gamma \int_{-\infty}^{\infty} dt e^{-i\omega t} \langle E(\mathbf{q}, t) E^*(-\mathbf{q}, 0) \rangle , \quad (2)$$

where $E(\mathbf{q}, t)$ and $\hbar\omega$ denote the magnetic energy density with the scattering vector \mathbf{q} and the energy transfer, respectively. γ is the \mathbf{q} - and ω -independent but polarization-dependent coefficient. We assume that γ is temperature-independent. $\langle \dots \rangle$ represents a thermal average. In the hydrodynamic condition,²⁷ Eq. (2) is transformed to

$$I(\omega) = \frac{\gamma\omega}{1 - e^{-\hbar\omega/k_B T}} \frac{C_m T D_T q^2}{\omega^2 + (D_T q^2)^2} . \quad (3)$$

Here D_T is a thermal diffusion constant which is given by

$$D_T = K/C_m , \quad (4)$$

where K is the magnetic contribution to the thermal conductivity. q is approximately equal to $|\mathbf{q}_0| \sin \theta/2$, where \mathbf{q}_0 and θ are the wave vector of the incident light and the scattering angle, respectively. In a high-temperature approximation, Eq. (3) can be written as the following Lorentzian curve

$$I(\omega) = \gamma' \frac{C_m T^2 D_T q^2}{\omega^2 + (D_T q^2)^2}, \quad (5)$$

where $\gamma' = k_B \gamma / \hbar$. Using Eq. (5), we can estimate the magnetic specific heat and the thermal diffusion constant from the integrated intensity and the half width at half maxima of the quasi-elastic scattering, respectively.

B. MAGNETIC SPECIFIC HEAT OF SPIN CHAIN WITH COMPETING EXCHANGE INTERACTIONS

We can calculate the magnetic specific heat using all energy levels in the spin system. Bonner and Fisher calculated magnetic susceptibility and magnetic specific heat in the spin system whose Hamiltonian is expressed by Eq. (1) with $\alpha = 0$ and $3 \leq N \leq 11$.⁸ They calculated all energy levels under the periodic condition by means of an exact diagonalization. Because a finite-size effect appears at low temperatures, physical quantities at $N \rightarrow \infty$ were estimated from an extrapolation. The magnetic specific heat of an infinite 1D AF chain with the nn AF exchange interaction has a broad maximum at $k_B T \approx 0.481J$.

In the case of $\alpha = 0.5$ (Majumder-Ghosh model), the ground state of the system with $4 \leq N \leq 8$ was studied analytically, and was revealed to be products of dimer states with double degeneracy.²⁸ This model was developed to the case of $N \rightarrow \infty$ and higher S .²⁹ An energy gap between the singlet ground and the triplet excited states opens in this case, while the magnetic excitation is gapless for $\alpha = 0$. Therefore, a phase transition takes place at $0 < \alpha < 1/2$. Tonegawa and Harada calculated the energy gap between the singlet ground and the triplet excited states numerically when $N \leq 20$,¹¹ and after this work, Okamoto and Nomura found that α_c at $N \rightarrow \infty$ is 0.2411 from their calculation when $N \leq 20$.¹²

We calculated all energy levels by means of the exact diagonalization for various α when $4 \leq N \leq 14$. We used a standard subroutine of the Householder method for a numerical diagonalization. We calculated the magnetic specific heat ($C_{m,N}$) for N spins and investigated $D_N = [NC_{m,N} + (N - 1)C_{m,N-1}]/(2N - 1)$ vs. N . D_N almost converges a value (*i.e.*, C_m) up to $N = 14$ at least when $T > 0.5T_{max}$. Here T_{max} is the temperature at which C_m has a maximum value $C_{m,max}$. Therefore we show D_N for $N = 14$ as C_m in Fig. 1a. T_{max} and $C_{m,max}$ decrease and the peak becomes broader with increasing α . We also calculate $C_m/C_{m,max}$ vs. T/T_{max} to obtain J and α from our observed data, and it is shown in Fig. 1b.

4. RESULTS AND DISCUSSION

Figure 2a shows polarized Raman spectra of CuGeO_3 at room temperature between -100 and 100 cm^{-1} strongly in the right-angle scattering geometries. The Raman spectra in the regions of $\omega > 0$ and $\omega < 0$ correspond to the Stokes and the anti-Stokes components, respectively. Since the intensity of the direct scattering is very strong, we cannot obtain Raman spectra in the region of $|\omega| < 7 \text{ cm}^{-1}$. The quasi-elastic scattering is strongly observed in the (c, c) polarization, while it is not observed in the offdiagonal geometries, *i.e.*, the (a, b) , (a, c) , and (c, b) ones. In the SP phase, we observed two-magnetic-exciton Raman spectrum below 250 cm^{-1} strongly in the (c, c) polarization.⁴ Thus, the magnetic fluctuations should appear strongly in the (c, c) polarization above T_{SP} , and we conclude that the quasi-elastic scattering of CuGeO_3 originates from the spin fluctuations in the spin system.

Figure 2b shows polarized Raman spectra between -100 and 500 cm^{-1} at room temperature in the right-angle $(b(c, c)a)$ and the quasi-back $(a(c, c)\bar{a})$ and $(a(c, c)\bar{a})$ scattering geometries. Because the Raman spectra in the $(b(c, c)a)$ and the $(a(c, c)\bar{a})$ scattering geometries were obtained with different scattering volumes, we cannot compare these scattering efficiencies directly. Then we normalized these Raman intensities by the integrated intensity

of the 181-cm^{-1} A_g phonon mode.⁴ On the other hand, since the $a(b, b)\bar{a}$ Raman spectrum was measured in the same experimental condition as the $a(c, c)\bar{a}$ spectrum, we can compare these intensities directly. The 181-cm^{-1} A_g phonon mode may have different intensities in the $a(b, b)\bar{a}$ and the $a(c, c)\bar{a}$ geometries. Two peaks at 114 and 221 cm^{-1} are B_{1g} modes, which are basically forbidden in this geometry. One can see a larger tail near the laser line and a stronger background at high-frequency region in the $a(c, c)\bar{a}$ geometry when compared with those in the $b(c, c)a$ geometry. We also observed a plasma line of the incident laser at -13.4 cm^{-1} in the quasi-back scattering geometry, while we did not observe it in the right-angle scattering geometry. These facts obviously indicate that the quasi-elastic scattering was strongly influenced by the direct scattering in the quasi-back scattering geometry. In the $b(c, c)a$ geometry, one can notice a crossover between the quasi-elastic scattering spectra and the incident laser line at $\pm 7\text{ cm}^{-1}$.

In our previous report,²⁰ we observed the plasma line at -13.4 cm^{-1} even in the right-angle scattering geometry, because the sample probably contains local strains and defects, and its quality was worse than that used in the present work. Moreover, since the ab face of the sample used in the previous work²⁰ was not as-grown but cut and polished, the effects of local strain on this surface and of strong diffused reflections of the laser light from this surface could not be avoided completely. Therefore, the Raman spectra in the previous report probably contained the weak component of the direct scattering, and we could not obtain the accurate integrated intensity of the quasi-elastic scattering especially at low temperatures.

We measured the temperature dependence of the low-frequency Raman spectra in the right-angle scattering geometry using the high-quality sample with as-grown ab surfaces. We think that we have done all we could do to avoid the effects of the direct scattering in the present measurements.

Figure 3 shows typical spectra of the quasi-elastic scattering at 250 , 120 , 50 , and 20 K. The intensity of the quasi-elastic scattering drastically decreases with decreasing temperature, and we did not observe the quasi-elastic scattering below T_{SP} . Since we did not

observe any asymmetric spectra above 20 K, the observed spectra are fitted to the following Lorentzian-type spectral function, instead of Eq. (3), using the method of least squares:

$$I(\omega) = \frac{k^2\Gamma}{\omega^2 + \Gamma^2} + \text{background}, \quad (6)$$

where Γ and k in Eq. (6) are the damping constant and the coupling coefficient, respectively. Comparing Eqs. (5) and (6), C_m and D_T can be evaluated from k^2 and Γ . The background is assumed to be expressed as $A\omega + B$. In the fitting, we use the Raman spectra of $|\omega| > 9 \text{ cm}^{-1}$, and then we can avoid the effects of the incident laser line near $\omega \sim 0$. Below 40 K, we could not fit the observed data because their intensities were very weak.

Van Loosdrecht *et al.* proposed that the origin of the low-frequency Raman spectra is the diffusive-type fluctuations in the four-spin time correlation functions.²⁴ According to Richards and Brya²⁵, this leads to a Gaussian-like low-frequency Raman spectrum. Then, we tried to fit the observed spectra to the following Gaussian-type spectral function:

$$I(\omega) = \frac{k_G^2}{\sqrt{2\pi}\Gamma_G} \exp\left(-\frac{\omega^2}{2\Gamma_G^2}\right) + \text{background}, \quad (7)$$

where k_G and Γ_G corresponds to k and Γ in Eq. (6). As seen clearly in Fig. 3, the Lorentzian-type spectral functions could reproduce the observed data much better than the Gaussian-type ones. Especially, the observed spectra near the incident laser line in the frequency region of $|\omega| \leq 15 \text{ cm}^{-1}$ did not fit to the Gaussian-type spectral function. This result indicates that the observed quasi-elastic Raman scattering does not originate from the diffusive-type four-spin fluctuations but from the spin-energy fluctuations.

We show the temperature dependence of Γ and k^2 above 50 K in Figs. 4a and 4b. As is drawn by a solid curve in Fig. 4a, Γ obeys $(T - T_{SP})^{1/2}$, and the same result was obtained in our brief report.²⁰ It is noted that Γ is proportional to D_T , and therefore to an inverse of a magnetic correlation length ξ^{-1} ($\Gamma \propto D_T \propto \xi^{-1}$).³¹ Although we did not observe the quasi-elastic scattering below 40 K, Γ seems to become zero around T_{SP} . Near the critical point, the thermal conductivity K which depends on short-range behavior of the system remains finite, while the magnetic specific heat C_m diverges.³² Then $D_T (= K/C_m)$ is predicted to vanish at T_{SP} .

Pouget *et al.*⁶ observed the structural fluctuations below about 40 K by means of X-ray diffuse scattering and they reported that the inverse correlation length of the structural fluctuations was proportional to $(T - T_{SP})^{1/2}$. Recent neutron-scattering studies^{33,34} showed that the magnetic correlation length agrees with the structural one near T_{SP} . The present result indicates that the obtained Γ of the quasi-elastic scattering above 50 K has the same temperature dependence. Then the inverse magnetic correlation length ξ^{-1} is described as $(T - T_{SP})^{1/2}$ not only just above T_{SP} but also at high temperatures.

Figure 5 shows k^2/T^2 above 50 K, which is proportional to C_m . As is seen in this figure, the data have some errors. Thus, we make smoothed data by a five point weighted mean (a solid curve), and compare them with theories. These errors are mainly caused by the difficulty in the temperature-dependence measurements. In the Raman-scattering measurements, it is not so easy to keep the exact alignment, because the spot of the incident laser line on the sample is moved by a thermal expansion of the cryostat.

A broad maximum is seen in the smoothed curve around 90 K. In Fig. 5, we show two theoretical magnetic specific-heat curves with $J = 237$ K and $\alpha = 0.30$ and with $J = 261$ K and $\alpha = 0.40$, which have maxima at 90 K. These curves are normalized in order that the maxima ($C_{m,max}$) of both the experimental and theoretical C_m agree with each other. Since the smoothed data exist between two theoretical C_m , J and α are roughly estimated at 250 ± 15 K and 0.35 ± 0.05 , respectively.

The competing- J model seems to explain the C_m of CuGeO_3 . However, the magnetic susceptibility in Ref. (1) is not in agreement with the theoretical one with J and α estimated in the present study. On the other hand, Riera and Dobry ($J = 160$ K and $\alpha = 0.36$)⁹ and Castilla, Chakravarty, and Emery ($J = 150$ K and $\alpha = 0.24$)¹⁰ have reported different J and α , and the theoretical magnetic susceptibility curves with their parameters agree with the observed magnetic susceptibility. However, as is shown by the dashed and dotted curves in Fig. 5, the corresponding theoretical magnetic specific-heat curves do not reproduce the measured one. Here we set $C_{m,max}$ by the value of the observed datum at 90 K. Then we conclude that we cannot find out the parameters which explain the observed magnetic

specific heat and the observed magnetic susceptibility simultaneously. This is a problem in the competing- J model.

Our α (0.35) is close to that of Riera and Dobry (0.36) and seems to be larger than α_c . This indicates that the energy gap remains finite even above T_{SP} . The energy gap above T_{SP} may be as large as $0.015J$ which was estimated by Riera and Dobry⁹ when $\alpha = 0.36$. However the finite gap in the uniform state has not been observed by any experiments. This is the second problem in this model.

The competing- J model is an interesting idea and is probably applicable to CuGeO_3 . However, this model cannot explain quantitatively all the experimental results. The problems may be solved by considering (i) interchain exchange interactions, (ii) temperature dependence of the exchange interactions, and (iii) structural fluctuations of the lattice dimerization.

These suggestions are due to the following reasons;

(i) In CuGeO_3 , the strength of the interchain interaction along the b axis is about 10% of that along the c axis,³ and it cannot be neglected. Riera and Koval suggested that the gap did not open in the uniform state even in the case of $\alpha = 0.36$ when the interchain interaction exists, because the interchain interaction changes the critical value α_c .³⁵

(ii) Because the lattice constant of CuGeO_3 changes strongly with decreasing temperature,^{7,36,37} J might depend on the temperature. It leads to a substantial effect on the temperature dependence of the magnetic susceptibility and the magnetic specific heat. When temperature dependence of J is taken into account, both the observed magnetic specific heat and the magnetic susceptibility might be explained simultaneously in terms of the competing- J model.

(iii) Pouget *et al.*⁶ observed the structural fluctuations of the lattice dimerization whose inverse correlation length is proportional to $(T - T_{SP})^{1/2}$ below about 40 K by X-ray diffuse scattering. Thus, the fluctuations may affect the magnetic specific heat and the susceptibility through a strong spin-lattice coupling.

Recently, Nakai *et al.*³⁸ obtained the magnetic specific heat up to 650 K by means of the

birefringence. The differential of birefringence with respect to temperature gives a magnetic specific heat. The temperature dependence of the magnetic specific heat shows a broad maximum around 80 K. Their result agrees well with ours.

5. CONCLUSION

We studied the quasi-elastic Raman scattering in CuGeO_3 , which is caused by spin-fluctuations. The quasi-elastic Raman scattering is observed only in the (c, c) polarization. The line shapes of the Stokes and anti-Stokes Raman scattering were well described by a Lorentzian curve around 0 cm^{-1} . This fact indicates that the quasi-elastic scattering originates from the fluctuations of energy density in the spin system. The temperature dependence of the half width at half maxima, which is proportional to ξ^{-1} , is well described as $(T - T_{SP})^{1/2}$. This is consistent with the results of the neutron-scattering studies. The temperature dependence of k^2/T^2 , which is proportional to the magnetic specific heat, was compared with the theoretical calculation by the competing- J model. The obtained $J = 250 \pm 15 \text{ K}$ and $\alpha = 0.35 \pm 0.05$ are different from those obtained in the magnetic susceptibility. We cannot find the parameters which explain the specific heat and the magnetic susceptibility at the same time. We suggested the reasons of the discrepancies between the experimental results and the competing- J model.

ACKNOWLEDGMENTS

This study is supported in part by the Research Fellowships of Japan Society for the Promotion of Science for Young Scientists and by a Grant-in-Aid for Scientific Research from the Ministry of Education, Science and Culture of Japan. The authors thank Mr. T. Nakai for useful discussion and sending their unpublished data, and also thank Prof. T. Ohtsuki for helpful discussion about theoretical calculations.

REFERENCES

1. M. Hase, I. Terasaki, and K. Uchinokura, Phys. Rev. Lett. **70**, 3651 (1993).
2. For review, J. W. Bary, L. V. Interrante, I. S. Jacobs, and J. C. Bonner, in *Extended Linear Chain Compounds*, ed. J. S. Miller (Plenum Press, New York and London, 1983) Vol. III.
3. M. Nishi, O. Fujita, and J. Akimitsu, Phys. Rev. B**50**, 6508 (1994).
4. H. Kuroe, T. Sekine, M. Hase, Y. Sasago, K. Uchinokura, H. Kojima, I. Tanaka, and Y. Shibuya, Phys. Rev. B**50**, 16468 (1994).
5. O. Kamimura, M. Terauchi, M. Tanaka, O. Fujita, and J. Akimitsu, J. Phys. Soc. Jpn. **63**, 2467 (1994).
6. J. P. Pouget, L. P. Regnault, M. Ain, B. Hennion, J. P. Renard, P. Veillet, G. Dhahlenne, and A. Revcolevschi, Phys. Rev. Lett. **72**, 4037 (1994).
7. K. Hirota, D. E. Cox, J. E. Lorenzo, G. Shirane, J. M. Tranquada, M. Hase, K. Uchinokura, H. Kojima, Y. Shibuya, and I. Tanaka, Phys. Rev. Lett. **73**, 736 (1994).
8. J. C. Bonner and M. E. Fisher, Phys. Rev. A**135**, 640 (1964). The Hamiltonian in this paper is defined by $2J_{BF} \sum_{i=1}^N (\mathbf{S}_i \cdot \mathbf{S}_{i+1})$.
9. J. Riera and A. Dobry, Phys. Rev. B**51**, 16098 (1995).
10. G. Castilla, S. Chakravarty, and V. J. Emery. Phys. Rev. Lett. **75**, 1823 (1995).
11. T. Tonegawa and I. Harada, J. Phys. Soc. Jpn.**56**, 2153 (1987).
12. K. Okamoto and K. Nomura, Phys. Lett. A**169**, 433 (1992).
13. H. Kuroe, K. Kobayashi, T. Sekine, M. Hase, Y. Sasago, I. Terasaki, and K. Uchinokura, J. Phys. Soc. Jpn. **63**, 365 (1994).
14. T. C. Kobayashi, A. Koda, H. Honda, C.U. Hong, K. Amaya, T. Asano, Y. Ajiro, M.

- Mekata, and T. Yoshida, *Physica* **B211**, 205 (1995).
15. S. Sahling, J. C. Lasjanias, P. Monceau, and A. Revcolevschi, *Solid State Commun.* **92**, 423 (1994).
 16. Y. K. Kuo, E. Figueroa, and J. W. Brill, *Solid State Commun.* **94**, 385 (1995).
 17. X. Liu, J. Wosnitza, H. v. Löhneysen, and R. K. Kremer, *Z. Phys.* **B98**, 163 (1995).
 18. S. B. Oseroff, S-W. Cheong, B. Akatas, M. F. Hundley, Z. Fisk, and L.W. Rupp, Jr., *Phys. Rev. Lett.* **74**, 1450 (1995).
 19. M. Weiden, J. Köhler, G. Sparn, M. Köppen, M. Lang, C. Geibel, and F. Steglich, *Z. Phys.* **B98**, 167 (1995).
 20. H. Kuroe, J. Sasaki, T. Sekine, Y. Sasago, M. Hase, N. Koide, K. Uchinokura, H. Kojima, I. Tanaka, and Y. Shibuya, *Physica* **B219-220**, 104 (1996).
 21. J. W. Halley, *Phys. Rev. Lett.* **41**, 1065 (1978).
 22. T. Sekine, M. Jouanne, C. Julien, and M. Balkanski, *Phys. Rev. B* **42**, 8382 (1990).
 23. I. Yamada and H. Onda, *Phys. Rev. B* **49**, 1048 (1994).
 24. P. H. M. van Loosdrecht, J. P. Boucher, G. Martinez, G. Dhalenne, and A. Revcolevschi. *Phys. Rev. Lett.* **76**, 311 (1996).
 25. P. M. Richards and W. J. Brya, *Phys. Rev. B* **9**, 3044 (1974).
 26. We used the same notation (*Pbmm*) as that in H. Völlenklee, A. Wittmann, and H. Howotny, *Monatsh. Chem.* **98**, 1352 (1967). The symmetry of this compound is *Pmma* in the standard orientation.
 27. B. I. Halperin and P. C. Hohenberg, *Phys. Rev.* **188**, 898 (1969).
 28. C. K. Majumder and D. K. Ghosh, *J. Math. Phys.* **10**, 1388 (1969).

29. I. Affleck, T. Kennedy, E. H. Lieb and H. Tasaki, Phys. Rev. Lett. **59**, 799 (1987), Commun. Math. Phys. **115**, 477 (1988).
30. I. Loa, S. Gronemeyer, C. Thomsen, R. K. Kremer, Solid State Commun. **99**, 231 (1996).
31. H. L. Swinney and H. Z. Cummins, Phys. Rev. **171**, 152 (1968).
32. L. Van Hove, Phys. Rev. **95**, 1374 (1954); B. I. Halperin and P. C. Hohenberg, Phys. Rev. **177**, 952 (1969).
33. M. Nishi, O. Fujita, J. Akimitsu, K. Kakurai, and Y. Fujii, Physica **B213&214**, 275 (1995).
34. K. Hirota, G. Shirane, Q. J. Harris, Q. Feng, R. J. Birgeneau, M. Hase, and K. Uchinokura, Phys. Rev. **B52**, 15412 (1995).
35. J. Riera and S. Koval, Phys. Rev. **B53**, 770 (1996).
36. J. E. Lorenzo, K. Hirota, G. Shirane, J. M. Tranquada, M. Hase, K. Uchinokura, H. Kojima, I. Tanaka, and Y. Shibuya, Phys. Rev. **B50**, 1278 (1994).
37. Q. J. Harris, Q. Feng, R. J. Birgeneau, K. Hirota, K. Kakurai, J. E. Lorenzo, G. Shirane, M. Hase, K. Uchinokura, H. Kojima, I. Tanaka, and Y. Shibuya, Phys. Rev. **B50**, 12606 (1994).
38. T. Nakai, M. Kubota, J. Yu, Y. Inaguma, M. Itoh, T. Kato, and K. Iio. Abstracts of the Meeting of the Physical Society of Japan, 1995 Sectional Meeting, Part 3, p. 187 and private communication with T. Nakai.

FIGURES

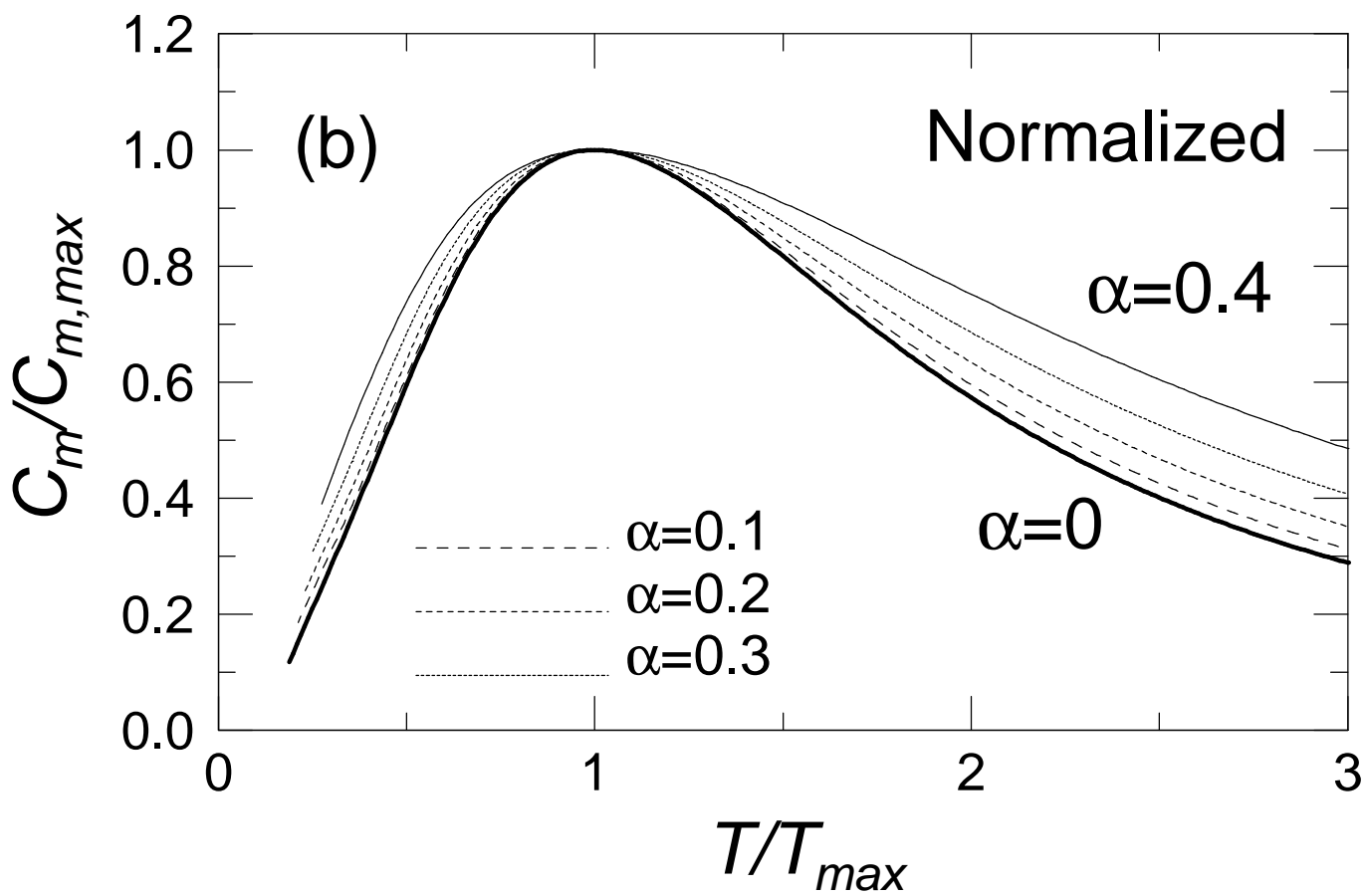
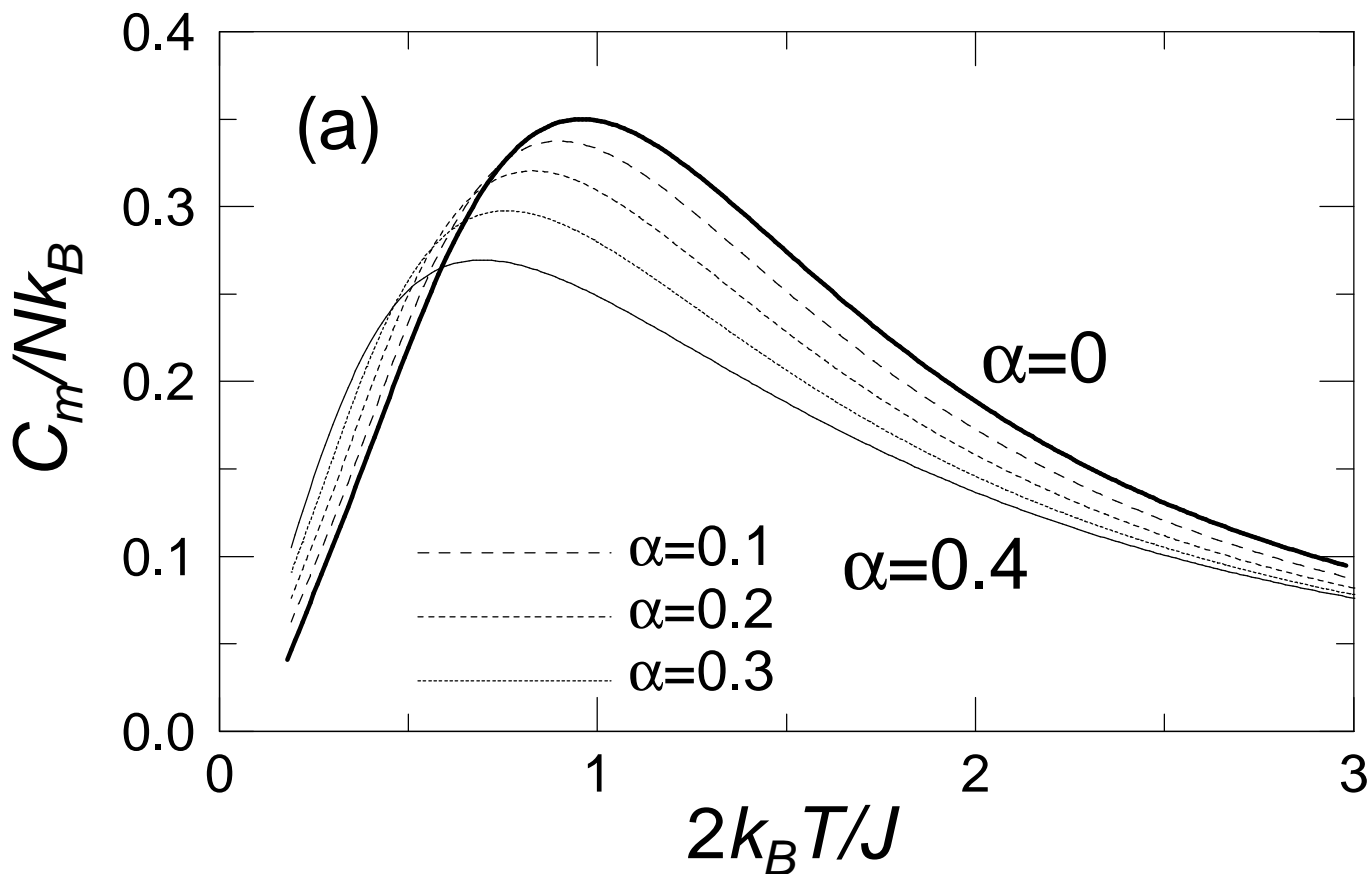
Fig. 1. Temperature dependence of the calculated magnetic specific heat for $\alpha = 0, 0.10, 0.20, 0.30,$ and 0.40 (a), and their normalized specific heat (b).

Fig. 2. Polarization characteristics of the Raman spectra between -100 and 100 cm^{-1} in CuGeO_3 in the right-angle scattering geometry at 300 K (a). Polarization characteristics of the Raman spectra between -100 and 500 cm^{-1} (b). The $b(c, c)a$ and $a(c, c)\bar{a}$ spectra in (b) are normalized by the intensity of the $181\text{-cm}^{-1} A_g$ phonon modes. Ar^+ denotes a plasma line of the Ar^+ ion laser at -13.4 cm^{-1} .

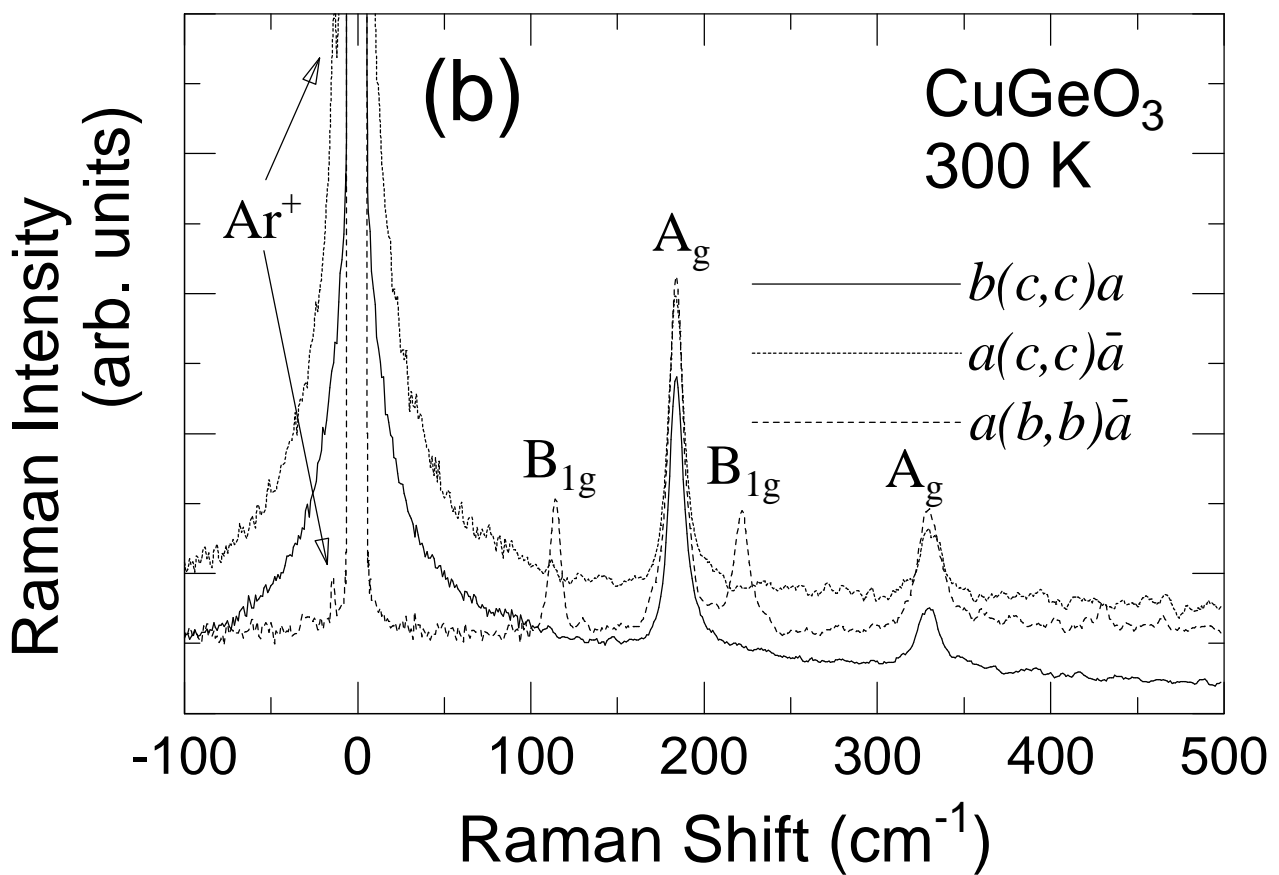
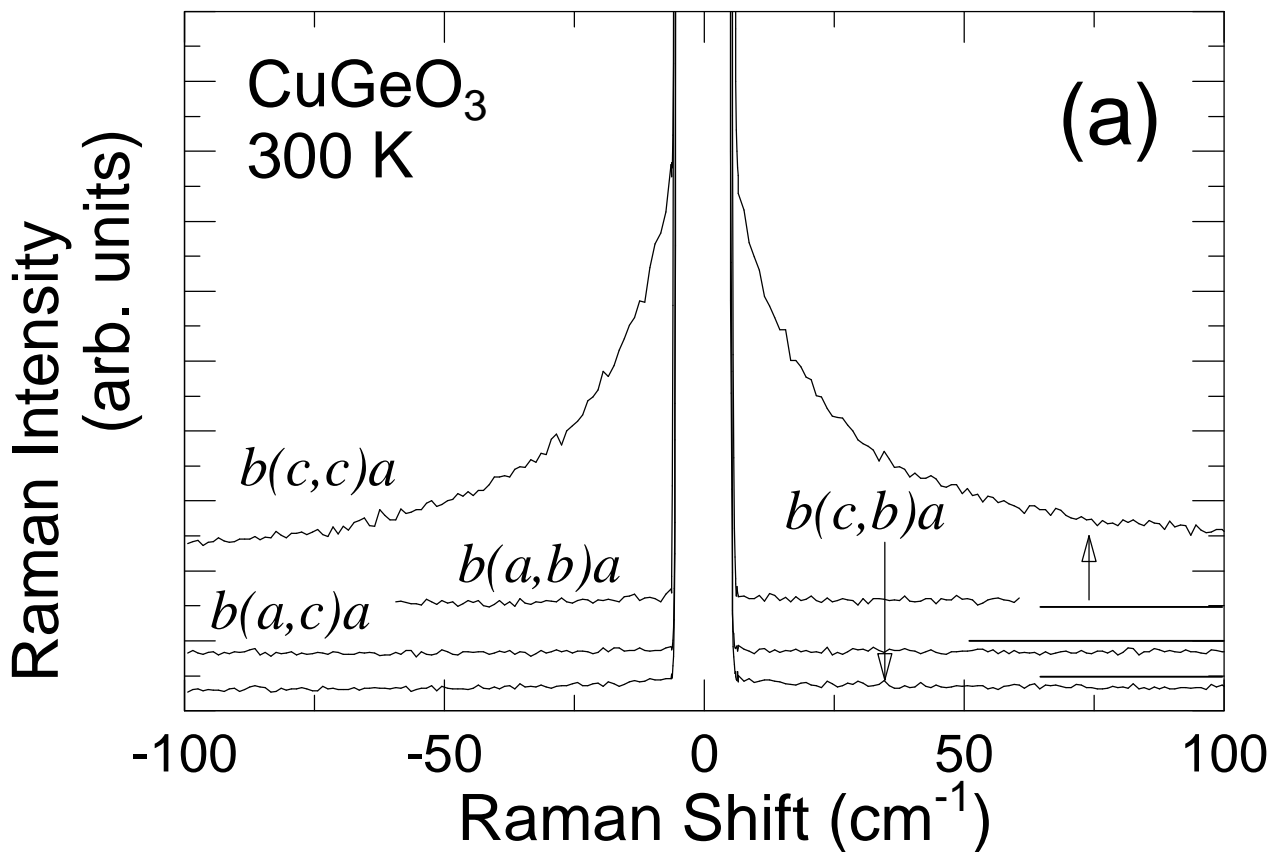
Fig. 3. Typical spectra of the quasi-elastic scattering in CuGeO_3 at 250 (circles), 120 (squares), 50 (triangles), and 20 K (diamonds). The solid and dashed curves denote Lorentzian curves and Gaussian curves, which are written in Eqs. (6) and (7), respectively.

Fig. 4. Temperature dependence of Γ (a) and k^2 (b) above 50 K in CuGeO_3 . The solid curve in (a) is proportional to $(T - T_{SP})^{1/2}$.

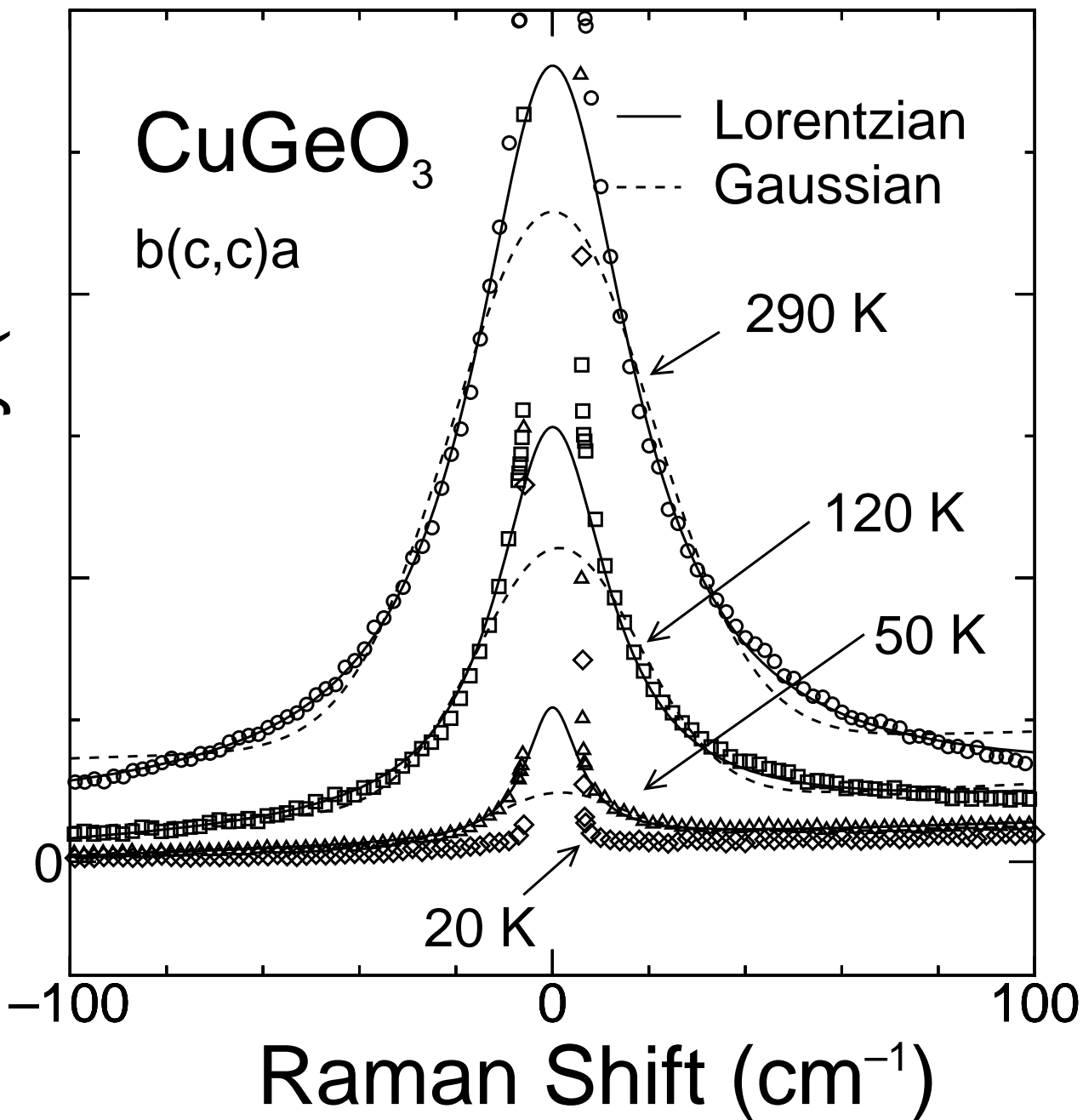
Fig. 5. Temperature dependence of k^2/T^2 above 50 K in CuGeO_3 , and the smoothed data. This figure also includes the calculated magnetic-specific-heat curves for $\alpha = 0.30$ and $J = 237 \text{ K}$, for $J = 261 \text{ K}$ and $\alpha = 0.40$, for the parameters of Riera and Dobry ($J=160 \text{ K}, \alpha = 0.36$) (Ref. 9), and for those of Castilla, Chakravarty, and Emery ($J=150 \text{ K}, \alpha = 0.24$) (Ref. 10). All the theoretical curves were normalized so that $C_{m,max}$ agrees with the observed datum at 90 K (see text).

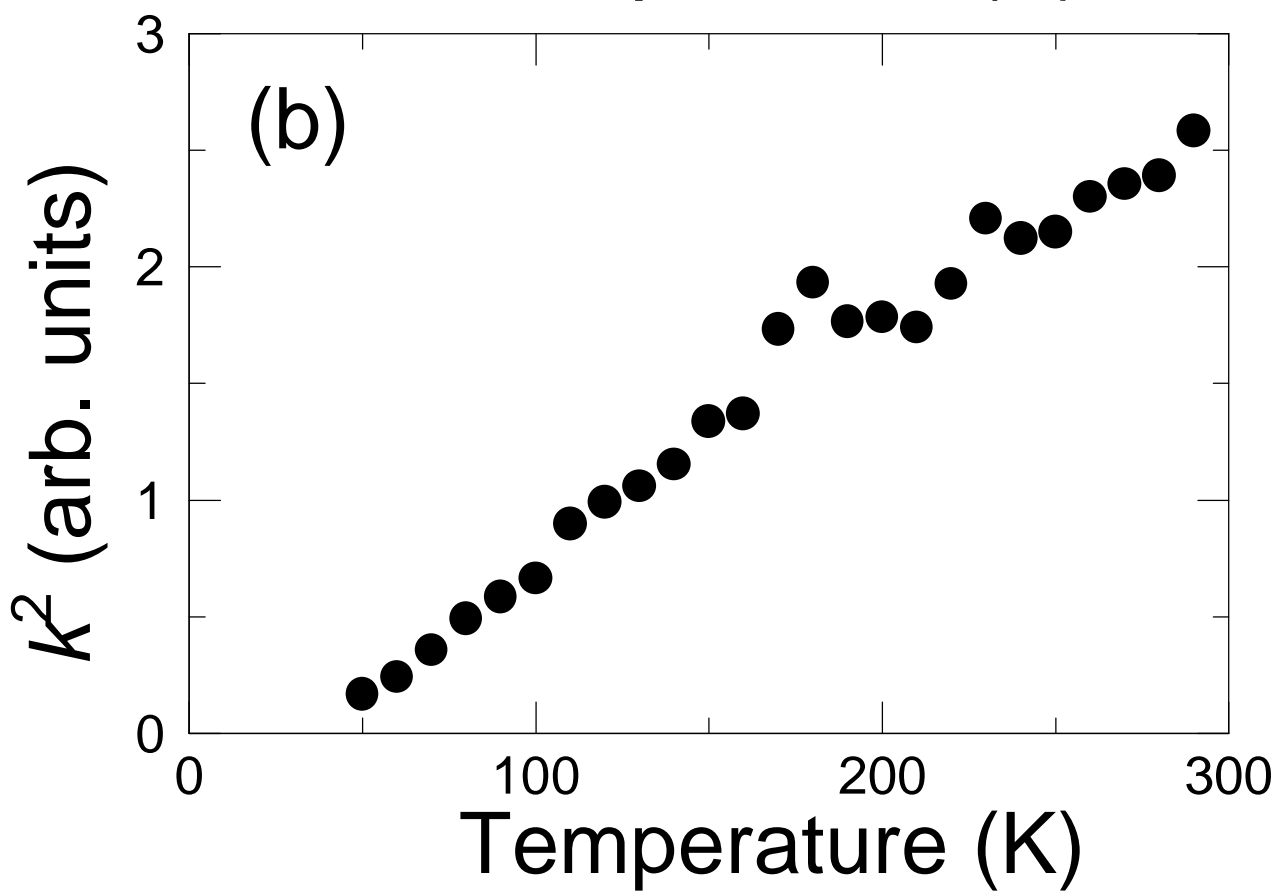
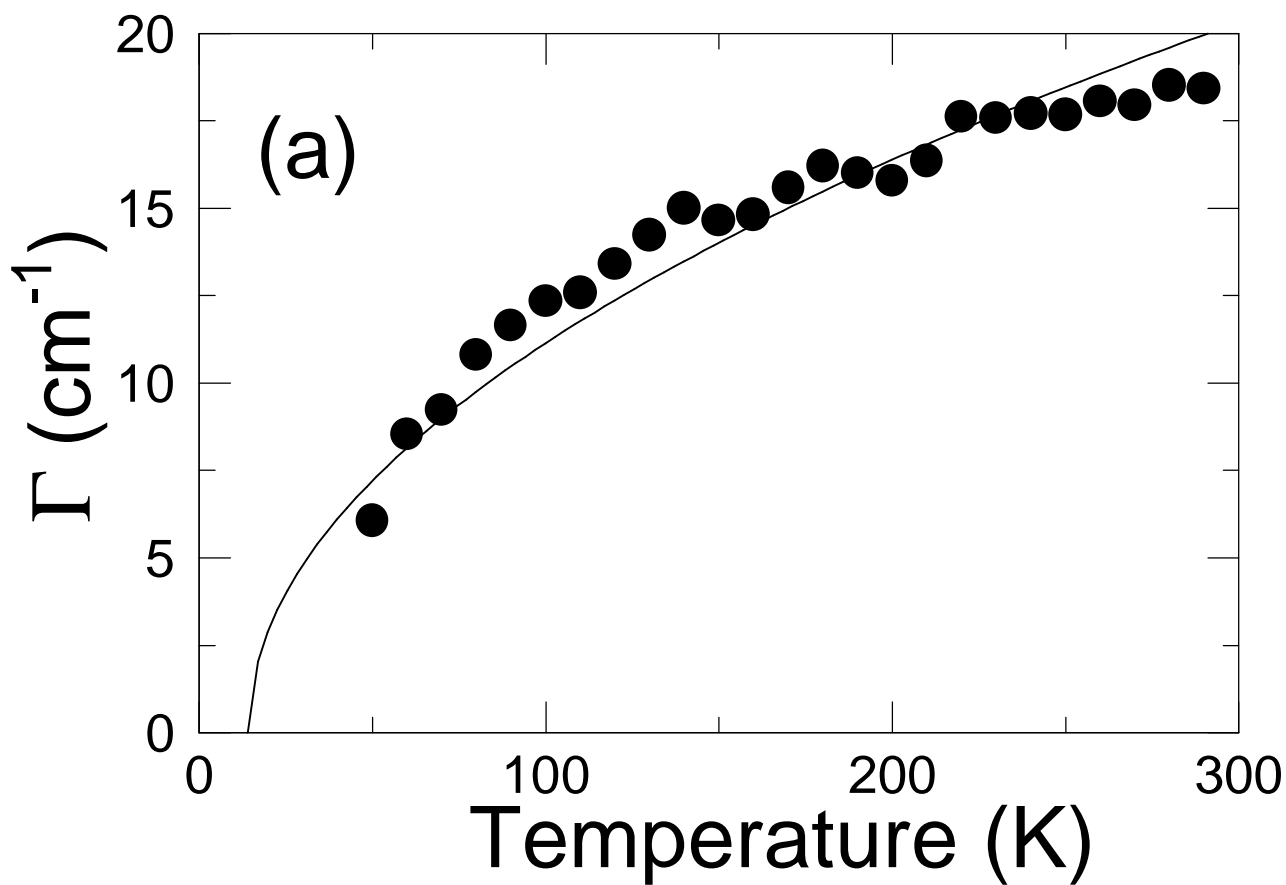


H. Kuroe *et al.* Fig. 1

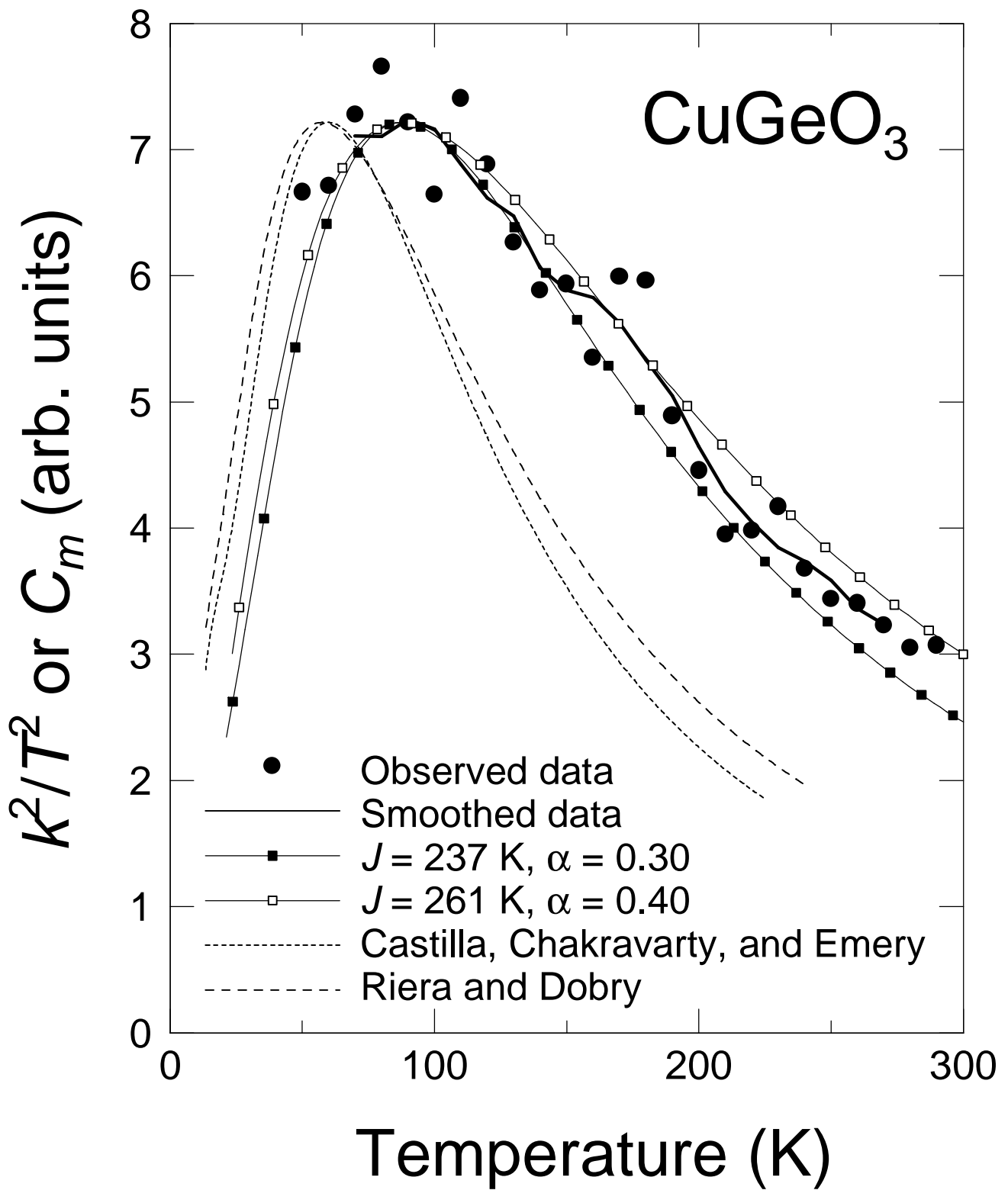


Raman Intensity (arb. units)





H. Kuroe *et al.* Fig. 4



H. Kuroe *et al.* Fig. 5